

**DISCOVERY OF NEW TARGETING AGENTS  
AGAINST GAPDH RECEPTOR:  
*IN SILICO* AND *IN VITRO* STUDIES**

**MUHAMMAD AMIRUL ASYRAF BIN NOH**

**UNIVERSITI SAINS MALAYSIA**

**2023**

**DISCOVERY OF NEW TARGETING AGENTS  
AGAINST GAPDH RECEPTOR:  
*IN SILICO* AND *IN VITRO* STUDIES**

by

**MUHAMMAD AMIRUL ASYRAF BIN NOH**

**Thesis submitted in fulfilment of the requirements  
for the degree of  
Master of Science**

**January 2023**

## ACKNOWLEDGEMENT

First and foremost, I would like to express my gratitude to Allah SWT. Thanks to His love and grace, I had the opportunity to conduct and finish this study. A very sincere gratitude to my supervisor – Dr Amirah binti Mohd Gazzali for her guidance and assistance throughout the term of my candidature. I am thankful for her advice and thoughtful insights, which had been of immense help in the completion of this research. I would also like to show my gratitude to Dr Siti Sarah Fazalul Rahiman, my co-supervisor for her magnanimous teachings and guidance, especially for the *in vitro* part of my study. I have learnt and benefitted much from her experience in this field. Additionally, I would like to give my thanks to Prof. Dr. Habibah A. Wahab for her advice and guidance in molecular dynamics.

Moreover, in completing this research, I had the pleasure of being introduced to molecular docking by Mr. Mohammad Gasem Mohammad Althiabat, a fellow postgraduate. My earnest thanks to him, and to my other fellow postgraduates for their support and help. Special thanks to Mr. Jusfaridan and Mr. Selvamani, assistant science officers from School of Pharmaceutical Sciences for their aid and contributions throughout the whole research progress.

Last but not least, I would like to dedicate my heartfelt gratitude to my parents, Noh Ibrahim and Aishah Khamis and my family members, Nur Erina Eliana Noh and Nur Shaherah Noh for their constant and never-ending support and encouragement in my research endeavours. Thank you.

## TABLE OF CONTENTS

<b>ACKNOWLEDGEMENT</b> .....	<b>ii</b>
<b>TABLE OF CONTENTS</b> .....	<b>iii</b>
<b>LIST OF TABLES</b> .....	<b>vi</b>
<b>LIST OF FIGURES</b> .....	<b>vii</b>
<b>LIST OF SYMBOLS</b> .....	<b>xii</b>
<b>LIST OF ABBREVIATIONS</b> .....	<b>xiv</b>
<b>LIST OF APPENDICES</b> .....	<b>xviii</b>
<b>ABSTRAK</b> .....	<b>xix</b>
<b>ABSTRACT</b> .....	<b>xxi</b>
<b>CHAPTER 1 INTRODUCTION</b> .....	<b>1</b>
1.1 General Introduction .....	1
1.2 Problem Statement .....	4
1.3 Objectives.....	5
1.3.1 General .....	5
1.3.2 Specific.....	5
<b>CHAPTER 2 LITERATURE REVIEW</b> .....	<b>6</b>
2.1 Tuberculosis .....	6
2.2 Current treatment of TB, MDR-TB and XDR-TB.....	8
2.3 Targeted drug delivery .....	12
2.3.1 Passive targeting.....	13
2.3.2 Active targeting .....	15
2.4 Target protein - GAPDH .....	19
2.5 <i>In silico</i> studies.....	24
2.5.1 Molecular docking.....	25
2.5.2 Molecular docking on GAPDH.....	28

2.5.3	Molecular dynamics .....	30
2.5.4	Molecular dynamics on GAPDH .....	31
2.6	<i>In vitro</i> studies .....	33
<b>CHAPTER 3 METHODOLOGY .....</b>		<b>37</b>
3.1	Overview of research methodology .....	37
3.2	<i>In silico</i> studies .....	38
3.2.1	Hardware details .....	38
3.2.2	Software details .....	39
3.2.3	Preparation of protein receptor for molecular docking .....	39
3.2.4	Preparation of ligands for molecular docking .....	39
3.2.5	Molecular dynamics .....	42
3.3	GAPDH Enzymatic Activity Assay .....	45
3.3.1	Chemical and Reagents .....	45
3.3.2	Equipment .....	45
3.3.3	Overview of the assay .....	45
3.3.4	Preparation of reagents .....	46
3.3.5	Determination of NAD reduction rate .....	48
3.3.6	Statistical analysis .....	49
<b>CHAPTER 4 RESULTS &amp; DISCUSSION .....</b>		<b>50</b>
4.1	Validation of docking studies (Preparations before docking) .....	50
4.2	Interaction of selected GAPDH inhibitors with GAPDH .....	52
4.3	Interaction of folic acid derivatives with GAPDH .....	57
4.4	Molecular dynamics simulations .....	69
4.4.1	Stability of the simulated complexes .....	70
4.4.2	Hydrogen bond analysis .....	75
4.4.3	Binding free energy (MM-PBSA) .....	77
4.5	GAPDH Enzymatic Activity Assay .....	83

<b>CHAPTER 5</b>	<b>CONCLUSION AND FUTURE RECOMMENDATIONS.....</b>	<b>87</b>
5.1	Conclusion.....	87
5.2	Recommendations for Future Research .....	88
<b>REFERENCES</b>	.....	<b>89</b>
<b>APPENDICES</b>		
<b>LIST OF PUBLICATIONS</b>		

## LIST OF TABLES

	<b>Page</b>
Table 2.1	Second-line antituberculosis drugs (TB/ Leprosy Sector, 2016). .....9
Table 2.2	Second-line antituberculosis drugs and their possible adverse effects (Ramachandran & Swaminathan, 2015)..... 10
Table 3.1	List of chemicals and reagents used in GAPDH enzymatic assay.....45
Table 3.2	List of equipment used in GAPDH enzymatic assay .....45
Table 4.1	Results obtained after docking of selected ligands (A-N) with GAPDH.....53
Table 4.2	Results obtained after docking of folic acid derivatives with GAPDH.....59
Table 4.3	Calculated average RMSD values for backbone protein atoms of different complexes..... 71
Table 4.4	Calculated average RMSD values for ligand atoms of different complexes..... 71
Table 4.5	Calculated average Rg values for different complexes.....73
Table 4.6	The occupancy of intermolecular hydrogen bonds formed in all complexes between GAPDH and the ligands alongside the hydrogen bond donor and acceptor atoms involved. .... 76
Table 4.7	Binding free energies (MM-PBSA) for GAPDH complexes from MD simulation trajectories (90–100 ns). Molecular docking values from AutoDock (ADT) 4.2 for the complexes are also included in the table. .... 78
Table 4.8	Percentage of GAPDH inhibition by types and differing concentration of ligands. ....84
Table 4.9	Results of one-way ANOVA test for the type of ligands on the inhibition percentage.....85

## LIST OF FIGURES

	<b>Page</b>
Figure 2.1	The enhanced permeation and retention effect (EPR) at infection sites. Adapted from “Local Bacterial Infection 2” figure template, by BioRender.com (2022a). Retrieved from <a href="https://app.biorender.com/biorender-templates">https://app.biorender.com/biorender-templates</a> ..... 14
Figure 2.2	Active uptake of therapeutic agent and nanoparticles in cells. Adapted from “Active Targeting of Cancer Stem Cells with Nanoparticles” figure template, by BioRender.com (2022b). Retrieved from <a href="https://app.biorender.com/biorender-templates">https://app.biorender.com/biorender-templates</a> ..... 16
Figure 2.3	Crystal structure of Glyceraldehyde-3-phosphate Dehydrogenase (GAPDH) from <i>Clostridium perfringens</i> SM101 that is made up of four monomers: chain A (blue), chain B (purple), chain C (orange), and chain D (green) along with NAD (cyan) as ligands. Image of PDB ID: 6FZI (Gómez et al., 2019) created with BIOVIA Discovery Studio 2019 (BIOVIA & Dassault Systèmes, 2019). .....20
Figure 2.4	Reduction of NAD to NADH by GAPDH.....34
Figure 3.1	Overview of research methodology .....38
Figure 3.2	The chemical structures of selected GAPDH inhibitors from literature. ....40
Figure 4.1	Superimposition of the crystallographic (blue) and docked (red) poses of NAD into the NAD binding domain of GAPDH. Image created with BIOVIA Discovery Studio 2019 (BIOVIA & Dassault Systèmes, 2019). .....50
Figure 4.2	2D diagram of crystal NAD-GAPDH complex. Image created with BIOVIA Discovery Studio 2019 (BIOVIA & Dassault Systèmes, 2019). .....51



Figure 4.3	2D diagram of docked NAD-GAPDH complex. Image created with BIOVIA Discovery Studio 2019 (BIOVIA & Dassault Systèmes, 2019). .....	52
Figure 4.4	Superimposed docked model of all 14 selected ligands and NAD (the co-crystallized ligand) at the NAD binding domain of GAPDH. Image created with BIOVIA Discovery Studio 2019 (BIOVIA & Dassault Systèmes, 2019). .....	53
Figure 4.5	2D diagram of ligand-protein complex of F (folic acid). Image created with BIOVIA Discovery Studio 2019 (BIOVIA & Dassault Systèmes, 2019). .....	57
Figure 4.6	Chemical structures of compound F and its derivatives. ....	58
Figure 4.7	Structure of folic acid. Separated into three parts: pteridine ring (black), <i>para</i> -aminobenzoic acid (red), and glutamic acid (blue).....	62
Figure 4.8	2D diagram of ligand-protein complex of F1. Image created with BIOVIA Discovery Studio 2019 (BIOVIA & Dassault Systèmes, 2019). .....	62
Figure 4.9	2D diagram of ligand-protein complex of F2. Image created with BIOVIA Discovery Studio 2019 (BIOVIA & Dassault Systèmes, 2019). .....	63
Figure 4.10	2D diagram of ligand-protein complex of F3. Image created with BIOVIA Discovery Studio 2019 (BIOVIA & Dassault Systèmes, 2019). .....	63
Figure 4.11	2D diagram of ligand-protein complex of F4. Image created with BIOVIA Discovery Studio 2019 (BIOVIA & Dassault Systèmes, 2019). .....	64
Figure 4.12	2D diagram of ligand-protein complex of F5. Image created with BIOVIA Discovery Studio 2019 (BIOVIA & Dassault Systèmes, 2019). .....	64
Figure 4.13	2D diagram of ligand-protein complex of F6. Image created with BIOVIA Discovery Studio 2019 (BIOVIA & Dassault Systèmes, 2019). .....	65

Figure 4.14	2D diagram of ligand-protein complex of F7. Image created with BIOVIA Discovery Studio 2019 (BIOVIA & Dassault Systèmes, 2019). .....	66
Figure 4.15	2D diagram of ligand-protein complex of F8. Image created with BIOVIA Discovery Studio 2019 (BIOVIA & Dassault Systèmes, 2019). .....	66
Figure 4.16	2D diagram of ligand-protein complex of F9. Image created with BIOVIA Discovery Studio 2019 (BIOVIA & Dassault Systèmes, 2019). .....	67
Figure 4.17	2D diagram of ligand-protein complex of F10. Image created with BIOVIA Discovery Studio 2019 (BIOVIA & Dassault Systèmes, 2019). .....	67
Figure 4.18	2D diagram of ligand-protein complex of F11. Image created with BIOVIA Discovery Studio 2019 (BIOVIA & Dassault Systèmes, 2019). .....	68
Figure 4.19	2D diagram of ligand-protein complex of F12. Image created with BIOVIA Discovery Studio 2019 (BIOVIA & Dassault Systèmes, 2019). .....	68
Figure 4.20	2D diagram of ligand-protein complex of F13. Image created with BIOVIA Discovery Studio 2019 (BIOVIA & Dassault Systèmes, 2019). .....	69
Figure 4.21	Plots of Root Mean Square Deviation (RMSD) values for the protein backbone atoms of the apo-GAPDH (black) and NAD/GAPDH (red), Folic acid/GAPDH (green), and F7/GAPDH (blue) complexes from initial structures throughout the 100 ns simulation as a function of time. Figure was produced using XMGRACE (version 5.1.19). .....	70
Figure 4.22	Plots of Root Mean Square Deviation (RMSD) values for the ligand atoms of NAD/GAPDH (black), Folic acid/GAPDH (red), and F7/GAPDH (green) complexes from initial structures	

	throughout the 100 ns simulation as a function of time. Figure was produced using XMGRACE (version 5.1.19).....	71
Figure 4.23	Radius of gyration (Rg) of the apo-GAPDH (black), NAD/GAPDH (red), Folic acid/GAPDH (green), and F7/GAPDH (blue) complexes from initial structures throughout the 100 ns simulation as a function of time. Figure was produced using XMGRACE (version 5.1.19). .....	72
Figure 4.24	Root mean square fluctuation (RMSF) of the apo-GAPDH (black) and NAD/GAPDH (red), Folic acid/GAPDH (green), F7/GAPDH (blue) and F5/GAPDH (yellow) complexes from initial structures throughout the 100 ns simulation as a function of time. Figure was produced using XMGRACE (version 5.1.19).....	74
Figure 4.25	The left structure shows the apo-GAPDH complex at the beginning of the MD simulation (at 0 ns) while the right structure shows the apo-GAPDH complex at the end of the MD simulation (at 100 ns). The red circle highlights the S-loop region. Image created with BIOVIA Discovery Studio 2019 (BIOVIA & Dassault Systèmes, 2019). .....	74
Figure 4.26	Number of hydrogen bonds formed between GAPDH and the ligands: A - NAD, B - Folic acid, C - F7 throughout the MD simulation. Figure was produced using XMGRACE (version 5.1.19). .....	75
Figure 4.27	MM-PBSA per residue decomposition for ligand-protein complexes of A - NAD/GAPDH, B - Folic acid/GAPDH and C - F7/GAPDH. All complexes were analysed at 100 ns of MD simulation. Figure was produced using gmx_MMPBSA. ....	80
Figure 4.28	2D diagram of ligand-protein complexes of A - NAD/GAPDH, B - Folic acid/GAPDH, C - F7/GAPDH. All complexes shown are at 100 ns of MD simulation. Image created with BIOVIA Discovery Studio 2019 (BIOVIA & Dassault Systèmes, 2019).....	82
Figure 4.29	Binding of A - NAD and B - F7 at the NAD binding site of GAPDH at 100 ns of their respective MD simulations. Image created with	

	BIOVIA Discovery Studio 2019 (BIOVIA & Dassault Systèmes, 2019). .....	83
Figure 4.30	Percentage of GAPDH inhibition by various concentrations of dimethyl fumarate (blue), folic acid (red), and F7 (green). n=3, triplicate. ....	84

## LIST OF SYMBOLS

%	percent
@	at
®	registered
°C	degrees Celsius
μg	microgram
μL	microlitres
μm	micrometre
μM	micromolar
Å	angstrom
fs	femtosecond
GB	gigabytes
GHz	gigahertz
K	Kelvin
kcal	kilocalories
kDa	kilodaltons
K <sub>i</sub>	Docking predicted inhibition constant
M	molar
mg	milligram
min	minutes
mL	millilitres
mM	millimolar
mol	mole
N	normality
nm	nanometre
ns	nanosecond

pH	potential of hydrogen
ps	picosecond
TM	trademarked
$\Delta G_{\text{bind}}$	binding free energy

## LIST OF ABBREVIATIONS

1,3-BPG	glycerate-1, 3-biphosphate
2D	two-dimensional
3D	three-dimensional
Abs	Absorbance
ACPYPE	AnteChamber PYthon Parser interfacE
ADP	Adenosine diphosphate
ADT	AutoDockTools
Ala	Alanine
AMBER	Assisted Model Building with Energy Refinement
ANOVA	Analysis of variance
Arg	Arginine
Asn	Asparagine
Asp	Aspartate
ATP	adenosine triphosphate
Av.	Average
BCG	Bacillus Calmette–Guérin
CADD	computer-aided drug design
CGenFF	CHARMM General Force Field
CHARMM	Chemistry at HARvard Macromolecular Mechanics
COVID-19	coronavirus disease 2019
CPU	central processing unit
cw-GAPDH	cell wall associated GAPDH
Cys	Cysteine
DECOMP	Decomposition
DNA	Deoxyribonucleic acid
DOPAL	3,4-dihydroxyphenylacetaldehyde
EDTA	Ethylenediaminetetraacetic acid
ELISA	enzyme-linked immunosorbent assay
EPR	enhanced permeation and retention
FDA	Food and Drug Administration
G3P	glyceraldehyde-3-phosphate

GAPA1	A1 isomer of chloroplastic glyceraldehyde-3-phosphate dehydrogenase
GAPDH	glyceraldehyde-3-phosphate dehydrogenase
Glu	Glutamine
Gly	Glycine
GOLD	Genetic Optimisation for Ligand Docking
GPUs	graphical processing units
GROMACS	GRoningen MAchine for Chemical Simulation
GROMOS	GRoningen MOlecular Simulation
HBC	high burden countries
HIRI	liver ischemia/reperfusion injury
His	histidine
HIV	human immunodeficiency virus
Ile	Isoleucine
LBDD	ligand-based drug design
Leu	Leucine
Lig	Ligand
LTS	long term support
Lys	Lysine
M. TB	mycobacterium tuberculosis
MD	molecular dynamics
MDR	multidrug resistance
MDR-TB	multi-drug resistant tuberculosis
MGL	Molecular Graphics Laboratory
MIC	minimum inhibitory concentration
min	minutes
MM-PBSA	molecular mechanics Poisson-Boltzman surface area
MPS	mononuclear phagocytic system
mRNA	Messenger ribonucleic acid
NAD	nicotinamide adenine dinucleotide
NADH	reduced nicotinamide adenine dinucleotide
NaOH	Sodium hydroxide
NHS	N-hydroxysuccinimide
NMR	nuclear magnetic resonance



NPT	fixed number of atoms, N, pressure, P, and temperature, T
NVMe	Non-Volatile Memory Express
NVT	fixed number of atoms, N, volume, V, and temperature, T
OA	oligoasthenozoospermia
PABA	<i>para</i> -aminobenzoic acid
PB	Poisson-Boltzman
PDB	Protein Data Bank
PDB ID	Entries identifiers in Protein Data Bank
PDBQT	Protein Data Bank, Partial Charge and Atom Type
PEG-PLA	polyethylene glycol-polylactic acid
Phe	Phenylalanine
PLGA	poly(lactic- <i>co</i> -glycolic acid
PME	Particle Mesh Ewald
PNM	Panax notoginseng mixture
Pro	Proline
Prot	Protein
PVDE	Polyvinylidene fluoride
QSAR	quantitative structure activity relationship
RAM	Random-access memory
Rg	radius of gyration
RMSD	root mean square deviation
RMSF	root mean square fluctuation
SBDD	structure-based drug design
Ser	Serine
TB	tuberculosis
TDC	Total decomposition contribution
Thr	Threonine
TIP3P	transferable intermolecular potential 3P
tRNA	Transfer ribonucleic acid
Tyr	Tyrosine
US	United States
VDW	van der Waals
VMD	Visual Molecular Dynamics
WHO	World Health Organization

XDR extensive drug resistance  
XDR-TB extensively resistant drug-resistant tuberculosis

## **LIST OF APPENDICES**

Appendix A      Calculation for inhibition percentage of folate derivatives

# **PENEMUAN AGEN PENYASARAN BAHARU TERHADAP RESEPTOR GAPDH: KAJIAN *IN SILIKO* DAN *IN VITRO***

## **ABSTRAK**

Tuberkulosis (TB) ialah salah satu daripada punca terbesar kematian di serata dunia yang disebabkan oleh sejenis agen berjangkit dan salah satu cadangan untuk mengatasi penyakit ini adalah dengan menggunakan kaedah penghantaran drug bersasar. Gliseraldehid-3-fosfat dehidrogenase (GAPDH), sejenis protein yang mempunyai pelbagai fungsi dan merupakan faktor virulens dalam mikroorganisma patogen, sesuai untuk dijadikan sasaran drug memandangkan ia telah dijumpai pada permukaan sel *Mycobacterium tuberculosis* (M. TB) baru-baru ini. Kajian ini memfokuskan pada pencarian molekul sasaran untuk GAPDH yang sesuai dan boleh digunakan dalam penghasilan agen antituberkulosis bersasar. Sebanyak 14 molekul yang dilaporkan mempunyai aktiviti *in vitro* dan/atau *in vivo* terhadap GAPDH atau kegunaan sebagai agen pensasar drug daripada kajian terdahulu telah diuji afiniti ikatan mereka terhadap reseptor GAPDH melalui teknik pengedokan molekul menggunakan AutoDock 4.2. Di antara 14 molekul ini, asid folik, NP-014428 dan CGP 3466 telah ditemui mempunyai afiniti ikatan paling baik dengan GAPDH. Seterusnya, 13 terbitan asid folik didok terhadap GAPDH. F7 (asid folik *N*-hidroksisuksinimida ester) dan F8 (asid folik  $\gamma$ -{[*tert*-butil-*N*-(2-aminoetil)]karbamate}) dijumpai mempunyai afiniti ikatan paling baik berbanding terbitan-terbitan asid folik yang lain. Simulasi dinamik molekul (MD) antara F7 dan asid folik dengan GAPDH dijalankan dengan menggunakan GROMACS 2021.2 bersama-sama NAD (nikotinamida adenin dinukleotida), ligan asal GAPDH sebagai agen kawalan positif. Jika dibandingkan dengan kompleks NAD/GAPDH, kompleks

asid folik/GAPDH merupakan kompleks yang paling stabil konformasinya tetapi paling lemah afiniti ikatannya manakala kompleks F7/GAPDH ialah kompleks yang paling tidak stabil konformasinya tetapi mempunyai afiniti ikatan yang paling kuat. Satu assai berenzim GAPDH turut diuji ke atas asid folik dan F7 dan didapati asid folik dan dimetil fumarat, sejenis perencat GAPDH yang juga merupakan agen kawalan positif dalam assai ini, menunjukkan kesan perencatan yang hampir sama terhadap GAPDH pada semua kepekatan (0-200  $\mu\text{M}$ ) tetapi secara umumnya F7 menunjukkan kesan perencatan yang lebih rendah sedikit daripada asid folik. Kesimpulannya, kedua-dua asid folik dan F7 menunjukkan potensi untuk dikembangkan sebagai agen pensasar GAPDH.

# DISCOVERY OF NEW TARGETING AGENTS AGAINST GAPDH RECEPTOR: *IN SILICO* AND *IN VITRO* STUDIES

## ABSTRACT

Tuberculosis (TB) is one of the leading causes of death due to a single infectious agent worldwide and one of the suggestions to overcome this disease is by using targeted drug delivery. Glyceraldehyde-3-Phosphate Dehydrogenase (GAPDH), a multifunctional protein and virulence factor in pathogenic microorganisms is suitable to be the designated drug target as it has been located on the cell surface of *Mycobacterium tuberculosis* (M. TB) recently. This research is focused on finding the suitable targeting molecules towards GAPDH that can be used for the development of targeted antituberculosis agents. Around 14 molecules with previously reported *in vitro* and/or *in vivo* activities against GAPDH or usages as targeting agents were assessed for their binding affinity through molecular docking technique using AutoDock 4.2. Among these 14 molecules, folic acid, NP-014428 and CGP 3466 were discovered to possess the best binding affinity with GAPDH. 13 derivatives of folic acid were then docked against GAPDH. F7 (folic acid *N*-hydroxysuccinimide ester) and F8 ( $\gamma$ -{[*tert*-butyl-*N*-(2-aminoethyl)]carbamate} folic acid) were discovered to possess the most favourable binding affinity among the folic acid derivatives. Consequently, F7 and folic acid were sent to undergo molecular dynamics (MD) simulations with GAPDH using GROMACS 2021.2 alongside NAD (nicotinamide adenine dinucleotide), the natural ligand of GAPDH as positive control agent. Compared to the NAD/GAPDH complex, folic acid/GAPDH complex has the most stable conformation but with the weakest binding affinity whereas F7/GAPDH complex having the most unstable conformation but has the strongest binding affinity.

A GAPDH enzymatic assay were also performed on folic acid and F7 and it was found out that folic acid and dimethyl fumarate, a GAPDH inhibitor and the positive control agent in this assay showed almost similar inhibitory effects on GAPDH at all concentrations (0-200  $\mu$ M), but F7 in general exhibited slightly lower inhibitory effects than folic acid. In conclusion, both folic acid and F7 shown their potential to be further developed as GAPDH targeting agents.

# CHAPTER 1

## INTRODUCTION

### 1.1 General Introduction

Tuberculosis (TB) is known to be one of the top causes of death worldwide (WHO, 2021a). From approximately 10 million people worldwide suffered from TB in the year 2020, 1.5 million were found dead due to the disease despite the availability of treatments and vaccines (WHO, 2021a). The causative agent of TB, *Mycobacterium tuberculosis*, (M. TB) spreads when it is expelled into the air through coughing by the infected person. Lungs are the main site of infection for TB (pulmonary TB) but the disease can also develop in other sites of the body (extrapulmonary TB) (Dheda et al., 2016).

The conventional treatment regimen for tuberculosis comprised of an intensive phase of four first-line antituberculosis drugs which are isoniazid, rifampicin, pyrazinamide and ethambutol that are administered for two months and followed by a continuation phase of isoniazid and rifampicin for the consecutive four months (Nahid et al., 2016). However, increasing spread of tuberculosis strains that are resistant to the first-line antituberculosis drugs (also known as multidrug resistant TB, or MDR-TB) necessitated the use of the second-line drugs which are less effective, thus, prompting their use for longer periods of time, which can last from nine months to 20 months (WHO, 2021a). In addition to the prolonged treatment period, second-line antituberculosis drugs such as cycloserine, ethionamide and kanamycin were also markedly more toxic than the first-line drugs (Horsburgh et al., 2015). Hence, there is a need to decrease the incident rate of MDR-TB concurrently with improving the present treatment regimen.



One of interesting approaches to improve drug therapy is via targeted drug delivery. This approach focused on increasing the amount of drug uptake at the target sites while decreasing the drug concentration at the non-target sites (Bareford & Swaan, 2007). Consequently, the drug is able to display its maximum effectiveness and exhibit fewer side effects due to lesser drug loss to non-target sites (Kazi et al., 2010; Manish & Vimukta, 2011). Targeted drug delivery is categorised into two main types: passive and active drug targeting. Passive targeting involves taking advantage of the changed environment of the targeted cells such as loosen blood vasculature and cell junction caused by the disease itself (Danhier et al., 2010). Meanwhile, active targeting involves conjugating a targeting moiety onto the drug or its vehicle to aim for upregulated target proteins at the target site when compared to other sites of the body (Clemons et al., 2018).

It should be pointed out that literature on targeted drug delivery towards TB are still lacking currently. Most research on M. TB cell-targeting focuses on the use of nanoparticles for passive targeting (Shivangi & Meena, 2018) or the phagocytic cells that are used by M. TB as their main host cells for active targeting (Guirado et al., 2013). Nevertheless, the recent finding of glyceraldehyde-3-phosphate dehydrogenase (GAPDH) on the cell surface of M. TB may pave the way to developing a targeting moiety that can be used for active targeting against M. TB (Malhotra et al., 2017). GAPDH has been known to play a huge role in the internalisation of lactoferrin and transferrin, iron-bearing proteins into the cytoplasm of M. TB (Boradia et al., 2014). If such internalisations can be applied similarly to antituberculosis drugs, this could lead to a new direction in the development of future treatment for TB.

This study seeks to uncover active small molecules that target GAPDH that will ultimately improve the delivery of antituberculosis drugs towards M. TB. *In silico* methods such as molecular docking and molecular dynamics simulations are conducted as part of the study to find out the suitable targeting molecule(s). Nowadays, *in silico* or computer-aided methods are frequently employed to calculate the potential bioactivity of suitable compounds for the eventual discovery of a lead compound (Seifert et al., 2003). In molecular docking, many possible orientations of a compound were generated at the binding site of a target protein and the orientation with the lowest binding energy is predicted to possess the best mode of binding to the binding site of the protein (Gagic et al., 2020). Meanwhile, molecular dynamics simulates the entire protein-ligand complex for further investigations into the temporal evolution of the molecular system (Ferreira et al., 2015; Gagic et al., 2020). Including computer-aided drug design in the process of drug discovery can save a significant amount of time and money (Seifert et al., 2003). After completion of the *in silico* studies, an *in vitro* study was performed using an enzymatic assay to verify the binding activities of the compounds discovered in the *in silico* studies.

## 1.2 Problem Statement

The increasing cases of MDR-TB or even extensively resistant drug-resistant TB (XDR-TB) worldwide shows a worrisome trend. Second-line drugs typically used for such case were known to be less effective than the first-line drugs with longer treatment periods and more significant side effects (Horsburgh et al., 2015). Discovery of new antituberculosis drugs have also been dismal, as not many drugs are approved as antituberculosis agents in the past 50 years, thus, necessitating a new direction to tackle this problem (Mazlan et al., 2021). Instead of finding new drugs, using targeted drug delivery approach, more specifically active targeting, towards the first-line drugs such as isoniazid or rifampicin may be a viable approach to improve the bioavailability of the drug and overcome drug resistance. GAPDH is a suitable protein target as it has been recently found on the cell surface of M. TB and also involves in internalising iron-bearing proteins (Boradia et al., 2014; Malhotra et al., 2017). Hence, in this study, suitable compounds that can be used as targeting agents against GAPDH were sought out and subjected to computational methods such as molecular docking and molecular dynamics simulations to find out their potential binding activity. The findings were later verified using experimental approaches via an enzymatic assay. It is hoped that the results from this study can be used to produce a promising targeting moiety that can be conjugated to a suitable antituberculosis drug to improve the delivery of the antituberculosis drug towards M. TB.

### **1.3 Objectives**

#### **1.3.1 General**

To elucidate suitable targeting molecule(s) towards GAPDH receptor of *M. tuberculosis* based on literature search using *in silico* and *in vitro* studies for the development of targeted antituberculosis agent.

#### **1.3.2 Specific**

- 1) To identify suitable targeting molecule(s) towards GAPDH receptor from 14 molecules identified through literature search through *in silico* molecular docking studies.
- 2) To investigate the mode of binding of the targeting agent on the targeted receptor and the thermodynamic stability of the complex through *in silico* molecular dynamic studies.
- 3) To verify the binding affinity of the potential targeting agent through *in vitro* GAPDH enzymatic assay.

## CHAPTER 2

### LITERATURE REVIEW

#### 2.1 Tuberculosis

Tuberculosis or commonly known as TB is an infectious disease caused by a group of microorganisms called *Mycobacterium tuberculosis* complex. The most prominent member of this group, *M. tuberculosis*, is the main causative of TB in humans. Other members of the complex such as *M. bovis*, *M. canetti*, *M. caprae*, *M. microti*, *M. mungi*, *M. orygis*, *M. pinnipedii* and *M. suricattae* are associated with TB in animals (Bajaj et al., 2021). However, *M. bovis* deserved a special mention as up to 10-15% of new TB cases in humans in developing countries are estimated to be caused by *M. bovis* (Ereqat et al., 2010). Based on studies on human bones from ancient graves and archaeological sites, it was deduced that TB has been present since more than 8000 years ago in ancient Near East and Europe (Buzic & Giuffra, 2020).

TB can affect different organs such as the lymph nodes, pleura, gastrointestinal tract, central nervous system, bones and genitourinary system but the main affected organ are the lungs (Houston & Macallan, 2014). This is because the lungs are highly exposed following inhalation of the droplets coughed out by TB patients (Carrol et al., 2001). In most cases, pulmonary TB develops slowly, with minimal symptoms until the disease is progressed moderately or far advanced. Most common symptoms are fever, cough and haemoptysis, which all start unremarkably but will increase in severity as the disease progresses (Popović Grle et al., 2013).

M. TB has shown the ability to successfully survive the host environment and escapes the host immune response. By having a portion of its cells dormant and not replicating, the whole population of M. TB is protected from eradication as most

antibiotics and immune responses will only target the actively replicating cells. This is a common reason for treatment failure or relapse of TB (Caño-Muñoz et al., 2018). Another important factor is its ability to utilise the host's resources for survival. For example, M. TB could utilize lactate that is abundant in host cells as their carbon source (Billig et al., 2017). In addition, M. TB also acquires iron from iron-loaded human proteins such as lactoferrin and transferrin (Banerjee et al., 2011).

Before the coronavirus disease 2019 (COVID-19) pandemic, TB was the main cause of death that is due to one sole infectious agent. In 2020, from approximately 10 million people that developed TB, 1.5 million deaths were recorded (WHO, 2021a). High frequency of exposure to M. TB such as close contact with TB patients or living in area infested with TB and impaired immune system due to certain diseases (e.g., HIV), conditions (e.g., malnutrition), or drugs (e.g., immunosuppressive drugs for organ transplants) can increase the possibility of contracting TB (Brett et al., 2020).

It is estimated that 80% of TB infections all over the world occur mostly in countries noted as “high burden countries” (HBC) by WHO. Although Malaysia is not included in the list of HBCs, Malaysia is being surrounded with countries that are - Indonesia, Myanmar, Philippines, Thailand and Vietnam (WHO, 2021b). In Malaysia, TB was estimated to have an incidence rate of 92 cases per 100,000 people in 2020, an increase from 75 cases per 100,000 people in 2010 (WHO, 2020; World Bank, 2020). It is believed that migrant workers from Bangladesh and Southeast Asian countries such as Indonesia and Myanmar are responsible for the increased TB prevalence in Malaysia (Mohidem et al., 2018). Nevertheless, the treatment success rate for new TB cases has increased from 73% in 2009 to 80% in 2019 (World Bank, 2019). However, the increment in Multiple Drug Resistance-Tuberculosis (MDR-TB) and Extensive Drug

Resistance-Tuberculosis (XDR-TB) cases both locally and globally is threatening the current available treatment options (Lange et al., 2018; Yao et al., 2021).

## **2.2 Current treatment of TB, MDR-TB and XDR-TB**

In Malaysia, the conventional treatment regimen of TB follows the regimen recommended by WHO (MaHTAS, 2012; WHO, 2021a). It comprises of two phases: the active phase and continuation phase. The active phase involves a two-month intensive phase of treatment with four antituberculosis drugs: isoniazid, rifampicin, pyrazinamide and ethambutol. The following continuation phase lasts for four months with two drugs; isoniazid and rifampicin (MaHTAS, 2012). This treatment regimen has been shown to be effective in eliminating TB in 90-98% of patients with drug-sensitive TB (Peloquin, 2002).

The long treatment duration is necessary due to the chronic nature of TB (Ramachandran & Swaminathan, 2015). The four antituberculosis drugs mentioned earlier, in addition to streptomycin have been used in combination as the first-line chemotherapy for TB for more than 40 years (Ma et al., 2010). Combination therapies are staple in TB treatment regimen to avoid the development of drug resistance in M. TB due to spontaneous mutation (Ramachandran & Swaminathan, 2015). However, the long treatment duration and high number of pills to be taken daily are among the challenges in ensuring patients' compliance towards treatment, as incompliance could lead to the development of drug-resistant TB (Bea et al., 2021; Ting et al., 2020).

Drug resistant TB are classified into several types. They are: (1) monoresistance, which refers to the resistance to a single type of first-line antituberculosis drug; (2) polydrug resistance, which means the resistance to more than one first-line antituberculosis drug other than isoniazid and rifampicin; (3) multidrug resistance

(MDR), which is the resistance to both isoniazid and rifampicin at the minimum; (4) rifampicin resistance, a resistance which may or may not include other antituberculosis; and (5) extensive drug resistance (XDR), which is the most difficult to be treated, as the resistance occurs on any drug from the fluoroquinolone group, plus one of the injectable second-line antituberculosis drugs, on top of the resistances mentioned in multidrug resistance (WHO, 2013). These types might overlap with each other and are not mutually exclusive. For example, more than 90% of strains that are resistant to rifampicin are also isoniazid-resistant (Seung et al., 2015). On that note, MDR-TB and XDR-TB strains are particularly worrisome among all drug resistant TB, considering their resistances towards both isoniazid and rifampicin that are the most powerful first-line antituberculosis drugs (Mitchison, 2000). Consequently, second-line antituberculosis drugs are typically used instead as the core of the treatment regimen for MDR-TB and XDR-TB (TB/ Leprosy Sector, 2016). Table 2.1 illustrates the second-line antituberculosis drugs and their groupings.

Table 2.1 Second-line antituberculosis drugs (TB/ Leprosy Sector, 2016).

Name of Group	Name of drugs	
A. Fluoroquinolones	Levofloxacin Moxifloxacin Gatifloxacin	
B. Second-line injectable agents	Amikacin Capreomycin Kanamycin Streptomycin	
C. Other core second-line agents	Ethionamide / Prothionamide Cycloserine / Terizidone Linezolid Clofazimine	
D. Add-on agents which are not included in the core multidrug resistance TB regimen	1	Pyrazinamide, Ethambutol, High-dose isoniazid
	2	Bedaquiline Delamanid
	3	<i>p</i> -aminosalicylic acid Imipenem-cilastatin



		Meropenem Amoxicillin-clavulanate Thioacetazone
--	--	---

The duration of treatment for MDR-TB is longer than for drug-sensitive TB. It can last from nine to 20 months (WHO, 2021a). For patients with XDR-TB on the other hand, the treatment could take up to 24 months (TB/ Leprosy Sector, 2016). The long treatment duration is attributed to the poor sterilising effects of the second-line antituberculosis drugs (Seung et al., 2015). Apart from that, second-line drugs are also notorious for their toxic nature as most of them can cause serious adverse reactions. Most of the commonly reported adverse effect are minor but several of the rare adverse effects could be quite deadly if not managed immediately (Ramachandran & Swaminathan, 2015). Table 2.2 lists some of the adverse effects that could be caused by the second-line antituberculosis agents.

Table 2.2 Second-line antituberculosis drugs and their possible adverse effects (Ramachandran & Swaminathan, 2015).

Name of drug	Adverse effects
Fluoroquinolones - Ofloxacin - Levofloxacin - Moxifloxacin	Central nervous system-related adverse effects - Delirium - Psychosis - Seizures Prolonged QT interval Arthropathy
Aminoglycosides - Amikacin - Capreomycin - Kanamycin	Nephrotoxicity Electrolyte abnormalities Ototoxicity
Ethionamide / Prothionamide	Gastrointestinal adverse effect Hypothyroidism
Cycloserine / Terizidone	Central nervous system adverse effects - Severe depression - Suicidal ideation
<i>Para</i> -aminosalicylic acid	Gastrointestinal intolerance Hypothyroidism Hypersensitivity reactions - Fever - Rash

	- Exfoliative dermatitis
Linezolid	Gastrointestinal toxicity Haematological toxicity - Myelosuppression Neurotoxicity - Peripheral neuropathy - Optic neuropathy
Clofazimine	Gastrointestinal adverse effects Dermatological adverse effects - Reddish-black/orange skin discoloration - Ichthyosis - Rash

Second-line antituberculosis drugs also have limited availability and exorbitant costs. The higher the level of resistance, the higher the cost of drug regimens needed for the treatment. For XDR-TB, the cost of drug treatment is tripled when compared to the cost of drug treatment for MDR-TB (Günther et al., 2015) and the cost of treatment for MDR-TB is more than triple the cost of treatment for drug-sensitive TB (Oh et al., 2017).

Although the disease burden of TB is high, this is not the topic of interest for many pharmaceutical and biotechnology companies as the returns are dismal to justify the cost and risk of researching and developing a new cure for TB (Trouiller et al., 2002). New drugs introduced to the market are more likely for the treatment of central nervous system disorders or cancers rather than neglected diseases like TB (Trouiller et al., 2002). However, there are three newly introduced anti-TB drugs that were recently approved: bedaquiline, approved by the US Food and Drug Administration (FDA) in 2012; delamanid, approved by the European Medicines Agency in 2013 and pretomanid, approved by the US FDA in 2019 (Angula et al., 2021). These drugs are approved for the treatment of resistant TB particularly MDR-TB and XDR-TB (Angula et al., 2021). This is great news considering that the last drug approved specifically for

TB was rifampicin in the 1970s (Ma et al., 2010; Seung et al., 2015). More innovative and attractive incentives should be offered by the governments around the world to encourage more discoveries, innovation and developments in TB treatment and eventually reach the goal of TB eradication.

### **2.3 Targeted drug delivery**

One of the fascinating approaches to improve the existing drug therapies is targeted drug delivery. The basic premise of targeted drug delivery focuses on increasing the amount of drug uptake at the target site while decreasing the amount of drug at other sites of non-interest (Bareford & Swaan, 2007). Thus, the maximum effectiveness of a drug can be demonstrated with lesser site effects due to reduced interactions and concentration at non-target sites (Kazi et al., 2010; Manish & Vimukta, 2011). Drugs employing this approach can be used in smaller quantities than the common dose to exert the desired therapeutic effects (Mazlan et al., 2021). This concept is not new – researchers in as early as 1906 have already envisioned targeted drug delivery which was named the “magic bullet”. Paul Ehrlich, the researcher in question, an immunologist from Germany imagined “magic bullets” as substances that would only exert their effects on the target and the target alone due to its exclusive affinity to that target and will apply minimal harm on the body due to the low affinity for non-target sites (Gradmann, 2011). Nanoparticles are often used as drug carriers for targeted drug delivery because they are stable, and their surface can be easily modified to attain disease-specific localisation and controlled release of drug (Singh & Lillard Jr, 2009). Targeted drug delivery can be divided into two broad categories: passive targeting and active targeting.

### **2.3.1 Passive targeting**

Passive targeting makes use of the unique variations in the environment of the target sites in comparison to other sites of the body and the physicochemical and pharmacological characteristics of the drug or drug carrier to deliver the drug to the target site (Attia et al., 2019; J. K. Patel & Patel, 2019). Passive targeting in TB treatment can be achieved in several ways. The first method took advantage of the fact that nanoparticles introduced in the human body will be rapidly engulfed through phagocytosis by macrophages or other phagocytes belonging to the mononuclear phagocytic system (MPS). Macrophages have been shown to accumulate nanoparticles in clearance organs such as the lungs, liver and spleen within minutes, fulfilling their role as the first-line of defence in the detection and elimination of foreign objects introduced into the host body (Gustafson et al., 2015). This is quite unfavourable for certain applications of nanoparticles such as cancer treatment but is advantageous for the treatment of infectious disease such as TB. Since the immune cells will be continually distributed to the infection sites, accretion of engulfed nanoparticles laden with antituberculosis drugs at sites of infection will occur (Clemens et al., 2012). In addition, the physicochemical characteristics of nanoparticles can also be modified to improve uptake by the macrophages. For example, highly charged or hydrophobic nanoparticles are swiftly opsonized by the MPS before being cleared through phagocytosis (Attia et al., 2019).

The enhanced permeation and retention (EPR) effect is implicated in the second method. The EPR effect was initially discovered by Matsumura and his team in 1986 and they found that nano-sized macromolecules and proteins accumulate more in tumours than non-tumours areas due to increased permeability of the surrounding tumour vasculature (hypervasculation) and decreased drainage to the lymphatic system

(Erickson, 2009; Matsumura & Maeda, 1986). Since increased vascular permeability is not unique to tumours and can occur in the inflamed tissues infected by bacteria, the EPR effect have surmised to occur in such tissues as well (Azzopardi et al., 2013). Figure 2.1 shows the EPR effect at infection sites. Size of the nanoparticles play an important role in determining their time of circulation in the body, as nanoparticles that are too small (less than 10 nm) will be quickly filtered by the kidneys and nanoparticles that are too large (larger than 100 nm) will be rapidly captured by the MPS (Danhier et al., 2010; Nakamura et al., 2016). Longer circulation times is important for tissue distribution, as this will help the accumulation of nanoparticles in the infected tissues, such as the lung tissues, as they have more chances to permeate those tissues (Baranyai et al., 2021).

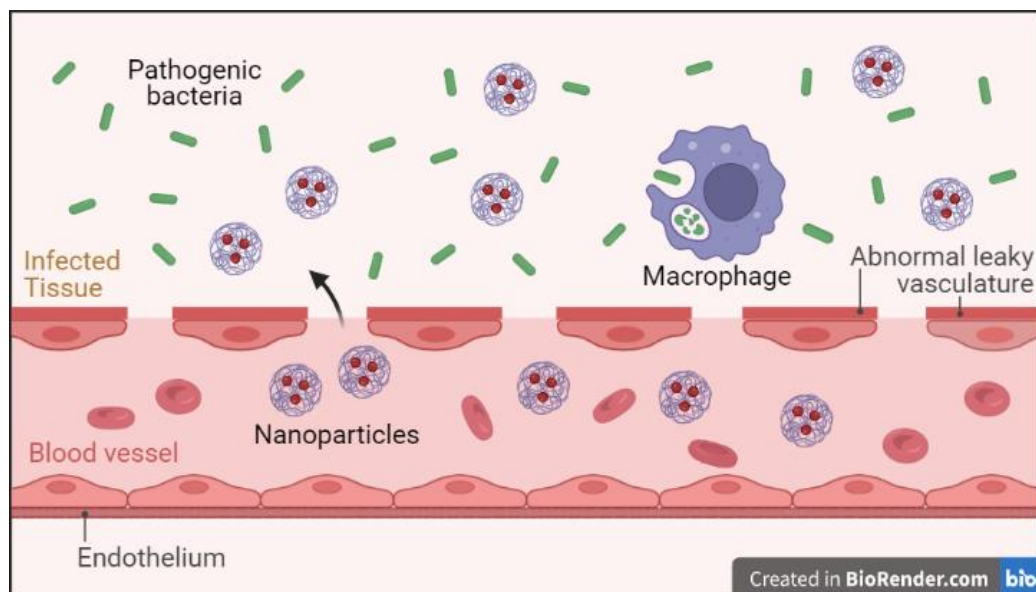


Figure 2.1 The enhanced permeation and retention effect (EPR) at infection sites. Adapted from “Local Bacterial Infection 2” figure template, by BioRender.com (2022a). Retrieved from <https://app.biorender.com/biorender-templates>

Several studies have employed passive targeting in their efforts to develop better treatments for TB. Raja *et al.* found that rifampicin enclosed in poly(lactic-*co*-glycolic acid) (PLGA) nanoparticles are more effective than rifampicin alone in killing BCG

bacteria within primary macrophages (Kalluru et al., 2013). Rani *et al.* produced nano-sized polymeric micelles from polyethylene glycol-poly(lactic acid) (PEG-PLA) copolymer to conjugate and encapsulate isoniazid and rifampicin respectively. The assembled micelles were remarkably better at reducing the occurrence of haemolysis as compared to isoniazid or rifampicin alone due to several factors that prevent direct contact with erythrocytes: 1) the presence of PEG on the surface of the micelle, 2) the encapsulation of rifampicin within the micelle, and 3) the location of the conjugated isoniazid near the core of the micelle. Additionally, minimum inhibitory concentration (MIC) of the micelle formulation was found to be approximately eight times lower than the MIC of the two individual free drugs (Rani et al., 2018). In another study reported by El-Ridy *et al.*, the authors reported that ethambutol encapsulated in niosomal formulations accumulated more in the mice lungs and the drug-loaded particles were retained for longer periods of time than free ethambutol. The same niosomal formulation has also caused a decrease in the number of bacteria in lung homogenates taken from guinea pigs (El-Ridy et al., 2015).

### **2.3.2 Active targeting**

Active targeting involves the conjugation or attachment of targeting moieties to a drug or its carrier which possess a binding affinity with a specific receptor expressed at the target site as seen in Figure 2.2. The target receptors should be upregulated by the target cells or the surroundings and present uniformly on all targeted cells to minimise or avoid delivery to non-target cells (Danhier et al., 2010). The binding of the targeting moiety on the cell surface receptor is usually followed by receptor-mediated endocytosis (Baranyai et al., 2021). The amount of drug delivered to target sites by active targeting are often much higher than by passive targeting or free drug (Attia et al., 2019). As M. TB are known to reside in MPS cells as their main host cells to survive

and multiply, the receptors of MPS may be used as the targets to increase the specificity of antituberculosis drugs (Guirado et al., 2013). Several types of MPS receptors have been identified and studied for their viability to be used as the potential targets in the active targeting of M. TB. Among the most studied are the mannose receptor, folate receptor and CD44.

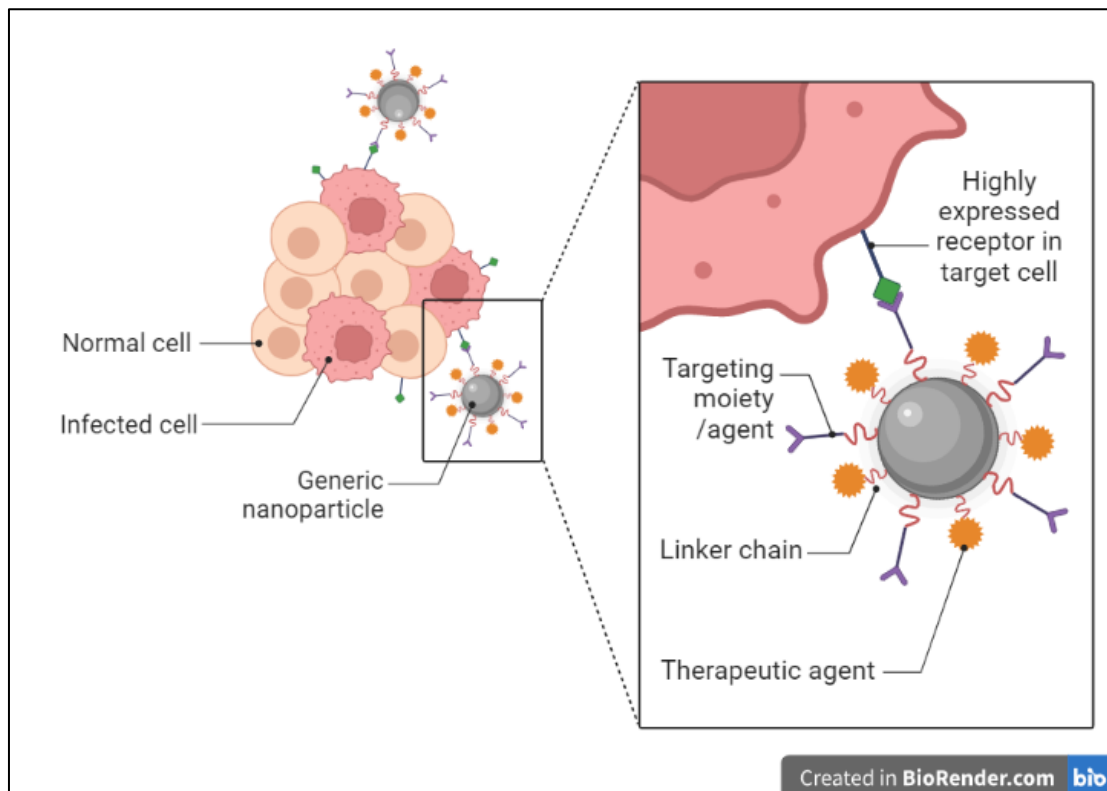


Figure 2.2 Active uptake of therapeutic agent and nanoparticles in cells. Adapted from “Active Targeting of Cancer Stem Cells with Nanoparticles” figure template, by BioRender.com (2022b). Retrieved from <https://app.biorender.com/biorender-templates>

Mannose receptor is a transmembrane glycoprotein that is expressed in the majority of tissue macrophages, dendritic cells and certain liver or lymphatic endothelial cells (Azad et al., 2014). Due to its high affinity towards sugars such as mannose and fucose as well as glycoproteins that bear sulphated sugars that were found in pituitary hormones, mannose receptor acts as a homeostatic receptor that regulate and clear excess glycoproteins conjugated with mannose and pituitary hormones in the

blood circulation by endocytosis or phagocytosis (Allavena et al., 2004; Lee et al., 2002). Since structures containing mannose are also present in the cell wall of numerous pathogens such as M. TB, these pathogens can interact with this receptor and subsequently be endocytosed by the macrophages. Additionally, the mannose receptor also took part in the adhesion and fusion of macrophages during granuloma formations, which is the characteristic symptom of TB (Azad et al., 2014; Silva Miranda et al., 2012). Granuloma is a structure formed by the host to contain the infection and eradicate M. TB (Silva Miranda et al., 2012). Hence, by targeting the mannose receptor, the drug/drug carrier conjugated with mannose can be internalised by the macrophages together with the M. TB and exert its intended effects on the offending pathogen. An *in vitro* study by Pi *et al.* showed that PEGylated graphene oxide that was conjugated with mannose were more readily internalized by macrophages than unconjugated PEGylated graphene oxide. When both graphene oxides were loaded with rifampicin and tested in intraepithelial lymphocytes taken from Rhesus macaques infected with M. TB, the PEGylated graphene oxide conjugated with mannose was observed to deliver a higher amount of rifampicin inside the CD14<sup>+</sup> macrophages when compared to the unconjugated PEGylated graphene oxide. Higher effective rifampicin concentration will lead to more effective eradication of intracellular M. TB (Pi et al., 2019).

Folate receptor is also being studied as a viable target for active targeting of M.TB (Baranyai et al., 2021). Due to its overexpression in cancer cells, the folate receptor has long been the target for the delivery of imaging and therapeutic agents for cancers (Fernández et al., 2017). Nevertheless, folate receptors can also be found overexpressed in other cells such as tumour-associated macrophages and activated macrophages involved in the progression of inflammatory and autoimmune diseases (Fernández et al., 2017; Xia et al., 2009). For infectious diseases especially TB however,



there are only few reported studies that utilised folate receptor as a target (Baranyai et al., 2021). Shah *et al.* developed rifampicin-loaded nanoemulsions decorated with chitosan and chitosan-folate conjugate that are able to be deposited deep within the lungs after nebulization to allow targeting of alveolar macrophages. Both nanoemulsions were found to be internalized by the macrophages and the viability of those macrophages were not harmed. However, the chitosan-folate decorated formulation produced a higher concentration of rifampicin intracellularly than the chitosan-only formulation. This can be explained that the chitosan-folate formulation utilised both mannose and folate receptors to be trafficked into the macrophages while the chitosan-only formulation utilised the mannose receptor alone for internalization into the cell (Shah et al., 2017).

Another interesting candidate for active targeting is CD44. CD44 is also a transmembrane glycoprotein, and it can be found expressed in keratinocytes, activated macrophages, fibroblasts, chondrocytes, and particular cancer cells (Montanari et al., 2018). The receptor can bind to a variety of glycoaminoglycans including hyaluronic acid (Sleeman et al., 1997). Hyaluronic acid has special characteristics in which it has distinct functions and distributions depending on its molecular weight. Hyaluronic acid with a molecular weight of higher than 1000 kDa can be found mostly inside healthy tissues in homeostatic conditions. It is also a major component of the extracellular matrix and can exhibit immunosuppressive behaviours (Baranyai et al., 2021; Lee-Sayer et al., 2015). However, tissue damage or infection can cause hyaluronic acid to break down to smaller fragments (less than 500 kDa), which will lead to inflammatory responses. Inflammatory conditions will cause upregulation of CD44 receptors in active immune cells, which allows them to bind and uptake hyaluronic acid. In non-inflammatory conditions, many immune cells do not bind to hyaluronic acid despite the

presence of CD44 receptors, except for the alveolar macrophages (Lee-Sayer et al., 2015).

The upregulation of CD44 receptors on macrophages during infection and the role that the receptor plays in the binding of M. TB with macrophages (like mannose receptors) are the reasons why CD44 is a promising target for active targeting (Leemans et al., 2003). Rossi *et al.* have used nanoparticles composed from low molecular weight hyaluronic acid to load isoniazid and rifampicin, two antituberculosis drugs together with verapamil, an efflux pump inhibitor (Rossi et al., 2019). The nanoparticles were designed to be inhalable to prevent cardiovascular toxicity by verapamil and improve the delivery towards alveolar macrophages (Pennock et al., 1991; Rossi et al., 2019). *Ex vivo* testing of the formulation with alveolar macrophages infected with drug-sensitive and drug-resistant strains of M. TB has shown favourable antituberculosis activities comparable to the free drugs. However, the encapsulated drugs showed better performance in decreasing the number of viable drug resistant TB strains than the non-encapsulated drugs (Rossi et al., 2019).

In addition to the previously described receptors, another receptor called Glyceraldehyde-3-phosphate Dehydrogenase (GAPDH) was recently discovered and reported to be present on the surface of M. TB. This will be described in the following subsection.

#### **2.4 Target protein - GAPDH**

Glyceraldehyde-3-phosphate Dehydrogenase (GAPDH) is widely known for its role in glycolysis as a catalyst for the conversion of glyceraldehyde-3-phosphate (G3P) to 1,3-biphosphoglycerate with the help of inorganic phosphate and nicotinamide adenine dinucleotide (NAD) (Nicholls et al., 2012). The resulting 1,3-

biphosphoglycerate and reduced nicotinamide adenine dinucleotide (NADH) from the reaction will be used in successive steps in glycolysis for adenosine triphosphate (ATP) generation (Muronetz et al., 2019). This protein is abundant and can be found in 10-20% of the total cellular protein (Tisdale, 2001). GAPDH normally takes the form of a tetramer that is made up of four identical subunits as can be seen in Figure 2.3. Each subunit is a polypeptide chain that is composed of 335 amino acids (Zhang et al., 2015).

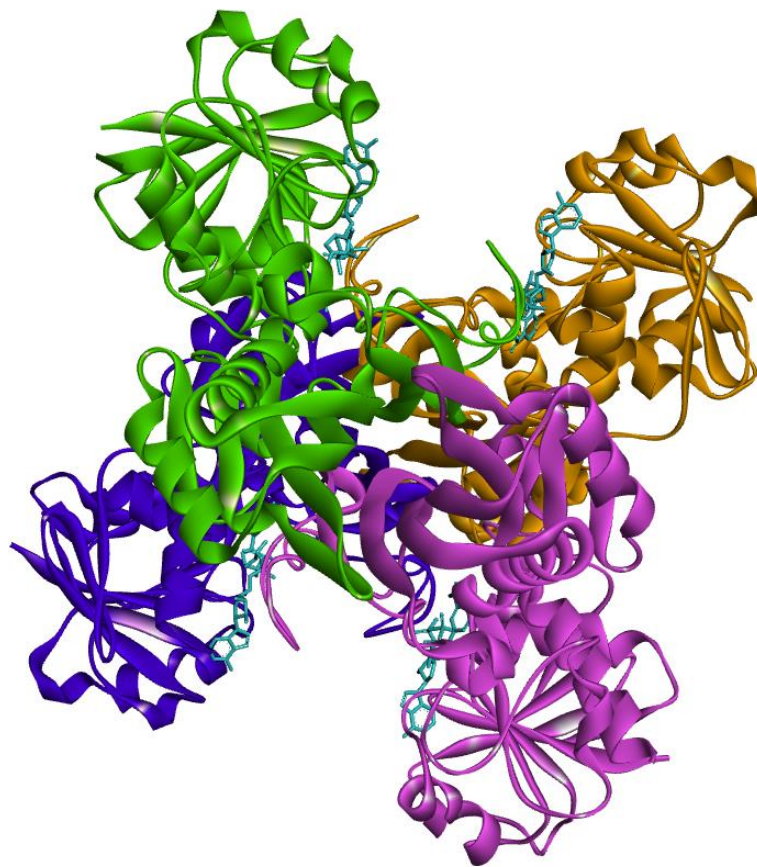


Figure 2.3 Crystal structure of Glyceraldehyde-3-phosphate Dehydrogenase (GAPDH) from *Clostridium perfringens* SM101 that is made up of four monomers: chain A (blue), chain B (purple), chain C (orange), and chain D (green) along with NAD (cyan) as ligands. Image of PDB ID: 6FZI (Gómez et al., 2019) created with BIOVIA Discovery Studio 2019 (BIOVIA & Dassault Systèmes, 2019).

Molecular studies show two main regions of interest, the NAD binding site and the G3P binding site, also known as the catalytic domain (Sirover, 1999). Any blockage or modifications to the NAD binding site can cause disruption in the glycolytic activity

of GAPDH (Kunjithapatham & Ganapathy-Kanniappan, 2018; Nagradova et al., 1972). For example, a study done by Herrmann *et al.* had found that the inhibitory activity of compound NP-014428 is due to its ability to act as a competitive inhibitor to NAD at the NAD binding site of GAPDH. As NAD functions as a catalyst in the glycolysis of G3P by GAPDH, this would result in lower GAPDH glycolytic activity. (Herrmann et al., 2015) Furthermore, even modifications to amino acids nearby the binding site may disrupt the glycolytic activity of GAPDH. A study by Malhotra *et al.* investigated the effect of mutations on several amino acids of M. TB GAPDH on its enzymatic activity. The N142S (asparagine to serine) mutant GAPDH barely preserved half of its enzymatic activity in contrast to the wild-type enzyme. No significant changes in the enzymatic activity were observed in the P295L (proline to leucine) mutant GAPDH. Even though N142 is not located within the NAD binding site, computational analysis proposed the N142S mutation causes instability to the neighbouring amino acids which include the NAD binding site and their interactions with a nearby helix, as N142 is a highly conserved residue in the GAPDH structure (Malhotra et al., 2017).

Additionally, besides its role as an important enzyme in glycolysis, GAPDH is also known to have numerous non-glycolytic functions that has led to its classification as a moonlighting protein (Kopeckova et al., 2020). For example, cytoplasmic GAPDH participates in intracellular trafficking between the endoplasmic reticulum and Golgi complex (Colell et al., 2009), the regulation of posttranscriptional mRNA expression and stability, and the cells' response to oxidative stress and hypoxia (Clemons et al., 2018; Colell et al., 2009). In the nucleus, GAPDH regulates the transcription of gene, export of tRNA and apoptosis, besides ensuring the integrity and stability of DNA. GAPDH that is present on the membrane surface is involved in endocytosis, membrane fusion and iron transport (Sirover, 2018).

GAPDH have been shown to act as a receptor for both transferrin and lactoferrin on the cell surface of different cells, and this includes macrophages (Sheokand et al., 2014). The actual binding site of transferrin and lactoferrin on GAPDH is not known but it is surmised that those iron binding proteins do not bind to the NAD nor the G3P binding site but instead a site different from them as a study showed that lactoferrin binding and enzymatic activity are independent of each other. (Malhotra et al., 2017) When there is a severe lack of iron in macrophages (e.g., due to intracellular infection by M. TB), the expression of membrane bound GAPDH will increase to boost the amount of transferrin and lactoferrin bound and taken inside the cells (S. Kumar et al., 2012; Rawat et al., 2012). Transferrin is an iron carrier protein found mostly in blood that is involved with iron chelation and transport in the body. Approximately 30% of transferrin in normal humans are sequestered with iron under normal situations to prevent toxicity caused by extracellular free iron (Sheftel et al., 2012). Meanwhile, lactoferrin is also an iron carrier protein that has many similar structures and functions as transferrin except the former is mainly found in the milk, secretions of exocrine glands (e.g., tears) and secondary granules of neutrophils (Baker et al., 2002; Sánchez et al., 1992). Cell surface GAPDH is not unique to human cells as previous studies have shown that GAPDH has also been identified on the cell surface of several microorganisms including M. TB (Kopeckova et al., 2020). As free iron ions are scarce extracellularly and intracellularly; M. TB have devised several methods to obtain iron from iron-carrier proteins vital of its continued existence. One of them is using siderophores, a low molecular mass iron binding compound that are secreted out from the bacteria to chelate iron from transferrin and lactoferrin before being re-uptake (K. Patel et al., 2018). However, it is discovered that cell-surface GAPDH on M. TB are also involved in the acquisition of iron by internalising bound host transferrin and

lactoferrin (Boradia et al., 2014; Malhotra et al., 2017). GAPDH's role as an iron-snatching virulence factor is also found in other microbes such as *Streptococcus agalactiae* and *Streptococcus pneumoniae* but they internalise haem or haemoglobin instead of transferrin or lactoferrin (Kopeckova et al., 2020; Yang et al., 2016). It can be surmised that a ligand that has high affinity towards GAPDH could bring in the conjugated antituberculosis drug directly into M. TB through this receptor, through which the efficacy of the drug can be improved.

Based on the upregulation of GAPDH expression on macrophages during infection and its role as a virulence factor for M. TB, GAPDH potentially serves as a viable candidate for designing suitable targeting agents for active targeting. A thorough search of relevant literature yielded no studies regarding the use of GAPDH as target protein for active drug delivery in M. TB, but Asthana *et al.* have done a similar study in *Leishmania donovani*, an intracellular parasite within macrophages. In hamsters infected with *L. donovani*, PLGA nanoparticles loaded with amphotericin B and decorated with lactoferrin were found to be more effective at inhibiting the growth of the parasite at the spleen by 88.61%. Undecorated amphotericin B-loaded PLGA nanocarrier and two commercial amphotericin B formulations (Ambisome® and Fungizone®) are less effective in the growth inhibition of *L. donovani*, which were reported as 64.40%, 68.8%, and 55.58% respectively. It is interesting to note that both decorated and undecorated amphotericin B-loaded nanoparticles have managed to significantly reduce the liver and kidney toxicities as compared to Ambisome® and Fungizone®. This is attributed to the slower release of amphotericin B, which helps to protect against toxicity to the organs mentioned (Asthana et al., 2015).

## 2.5 *In silico* studies

The discovery, design and development of a new drug is not a simple task. It is an expensive and time-consuming process that can take up to several years of research and development (Swaan & Ekins, 2005). In this process, the discovery of a lead compound is often the most crucial part. Lead compounds would primarily be discovered through high-throughput screening of chemical compounds on a specific receptor of interest (Mazza et al., 2002). Interestingly, the emergence of computer-aided or *in silico* methods to evaluate the potential bioactivity of compounds of interest have reduced the number of compounds to be tested experimentally. Hence, *in silico* methods have been used to complement or even substitute high-throughput screening. Using this approach, *in silico* methods can reduce the amount of time and cost spent during the process of drug discovery and development (Seifert et al., 2003).

There are two major approaches in computer-aided drug design (CADD): ligand-based drug design (LBDD) and structure-based drug design (SBDD). LBDD is undertaken when the 3D structure information of the target receptor is not available. This approach depends on the knowledge of the existing ligands that bind to the target site (Aparoy et al., 2012). Hence, similar yet more potent ligands can be designed and developed. (Seifert et al., 2003) Some of the methods included in LBDD are ligand-based virtual screening, similarity searching, quantitative structure activity relationship (QSAR) and pharmacophore modelling (Gagic et al., 2020). Meanwhile SBDD is built upon the premise where the structural information of the target site is known and being referred to for the development of its ligand (Aparoy et al., 2012). This allows for the virtual screening of ligands that fit or complement the target site (Seifert et al., 2003). Some of the methods included in SBDD are structure-based virtual screening, molecular docking, and molecular dynamics (Gagic et al., 2020). In this study, molecular docking